



Adaptive Optics system-box for the QKD transportable ground station at IAC

Joan Torras^a, Jorge Socas^a, Luis Fernando Rodríguez^a, Iciar Montilla^a, Alex Oscoz^a, Ángel Alonso^a, Elena Reyes^a, Serena Maroquin^a, and Noelia Martínez^b

^aInstitute of Astrophysics of the Canary Islands, La Laguna, España

^bAustralian National University ANU, Australia

ABSTRACT

Free space optical communications implementing QKD protocols demand sensors with very high signal to noise ratio, compatible with the reduced size of a single-mode fiber core. The use of adaptive optics allows high data throughput links, by correcting the aberrations generated by atmospheric turbulence. In this paper we present the design of an adaptive optics (AO) system-box to correct for daytime and nighttime atmospheric turbulence. The system will be small enough to be implemented at the Nasmyth focus of a transmitter/receiver 70cm-aperture telescope used as a Transportable Optical Ground Station in urban sites or LEO links scenarios or in the OGS at Teide Observatory 1 meter-aperture telescope. The setup will correct for aberrations based on a plenoptic wavefront sensor camera. The optical performance of the system will be analysed, together with simulations of turbulence to estimate the increase on the coupling from free-space to SMF.

Keywords: transportable optical ground station, adaptive optics, lasercoms, single mode fiber coupling, plenoptic wavefrontsensor, QKD, BB84

1. INTRODUCTION

The recent progress in Quantum computer has caused the developing of alternative cryptographic systems, that allow to raise up the security level in the communications. Quantum Key Distribution (QKD), based on quantum mechanics, has provided a strategy to detect the presence of intruders in the communications channels and in that way certify the security of the channel. All the current Quantum Key Distribution methods are based on the transmission of single photons, either through entangled photons or prepare and measure methods. In quantum cryptography, the transmitter, known as Alice, and the receiver, known as Bob (as were first mentioned in the 1978 paper written by a group of MIT researchers¹), exchange a key by using two communication channels: the first is the quantum channel that can be the optical fiber or free space, and the second is the classical channel that is the public channel that could be internet or also free-space.

Further author information: (Send correspondence to J.T)

J.T.: E-mail: joan-torras@iac.es

L.R.R.: E-mail: lrr@iac.es

Typically exist two different approaches to QKD, in order to generate secret key: Discrete Variable QKD and Continuous Variable QKD.² The differences are summarized in the Table 1.

Table 1: Different approaches to QKD.

DV-QKD	CV-QKD
Long networks (40 and 100 km)	short networks
Based on single photons homodyne detection technology	Based on mature optical components
Less suited for integration in telecom networks	Easy to integrate in existing equipments
Needs dedicated optical fibers for quantum channel	Higher secret key rates
Mature technology	No need for dedicated optical links
Protocols: ³ BB84, B92, SARG04, E91	Protocols: ³ GG02

QKD has been experimentally demonstrated in fibers,⁴ in free space⁵ and satellites. Nevertheless the losses of the terrestrial fiber optical networks and the difficulty to deploy, limit the distribution over just a few hundred of kilometers. Also it must be considered that an optical fiber has some level of birefringence, in consequence modifying the polarization state of the transmitted signal. This gap seems to be covered by Quantum Key Distribution over a free space channel.

Free Space optical communications have been gaining relevance in the telecommunications field in recent years, because provide larger bandwidth and narrower beams than radiofrequency.⁶ The systems are more compact and have higher power efficiencies. Although on the other hand, meteorological phenomena can eventually make those communications impossible, as a cloud-free line of sight is needed for the optical link to successfully establish a QKD. In case of local cloud coverage, the problem may be solved targetting another (cloud free) customer or site (redundancy network).

The Institute of Astrophysics of the Canary Islands is designing and developing a Transportable Optical Ground Station TOGS with ease of movement and portability, in order to act as a transmitter or a receiver of QKD over free space optical communications channel, and with Adaptive Optics as a solution to compensate the atmospheric turbulence and improve the coupling efficiency.⁷

This Adaptive Optics solution has been designed as a modular AO box to be attached to the telescope body (an $f/12$ Ritchey-Chrétien with an aperture of $70cm$), in particular to the Nasmyth focus. The system will actively compensate the aberrations introduced by the turbulent atmosphere during the operation of the ground station. The compensation given by the AO system is expected to provide the necessary gain in efficiency coupling to an SMF fiber necessary for quantum key distribution in optical communications. Other systems with active compensation for transportable configurations have been developed in the past,⁸ but they use a Shack-Hartmann (SH) wavefront sensor. In our case, a plenoptic camera will be used as a wavefront sensor. Previous work⁹ shows an increase in coupling efficiency, in particular when a plenoptic camera is used as a wavefront sensor (WFS) for sensing the atmospheric turbulence during a daytime ground to ground link, that results to be the most demanding scenario for a long range link.

2. SYSTEM OVERVIEW

The transportable optical Ground Station system consists of a system that includes the capabilities of both Alice and Bob, that is, it could behave as Alice or Bob, depending on the scenario used. It should be able to obtain a quantum-secured key known only to both, using BB84 protocol discrete variable as baseline.

BB84 is the most widely implemented discrete variable quantum key distribution protocol. It was developed by Charles Bennet and Gilles Brassard in 1984.¹⁰ The fundamental concept of this protocol is that Alice randomly selects a series of q-bits, then she sends them into a quantum channel in the form of photons to Bob in order to create a secret key. It will be encoding either on its polarization or phase.

Transportability is the key feature of the system, the TOGS is transportable using commercially available transport systems. The TOGS designed and developed by IACTEC, include functionality for terrestrial and bidirectional LEO to ground links. Terrestrial links include communications between buildings, mountains, islands, or any other kind of “horizontal” link between two ground stations, and LEO links include both ground-to-satellite or satellite-to-ground, in order to share quantum keys between both.

We split the system design in 3 parts: The mechanical design, that includes the dome, holders, trailers and all the transportable parts; the optical subsystem, that includes the telescope, “Alice Box“ and “Bob-Box”; and the electronics subsystem that include the data post processing. “Alice-Box” includes the sender of the quantum key, and “Bob-Box” includes the receiver of the quantum key. These boxes share parts (i.e. the telescope). Alice and Bob are modular boxes, with the optical components inside and are mounted on the Nasmyth focus of the telescope.

During transmission of photons, they are exposed to different effects in the atmosphere, namely: absorption, scattering and refractive-index fluctuations due to atmospheric turbulence.¹¹ These interactions and losses in the optical channel have a significant and major influence on the probability to detect photons emitted by Alice and received by Bob. Absorption and scattering as well as beam divergence attenuate the received laser beam power, but the stronger deterioration of the performance of the communication is produced by the atmospheric turbulence, introducing phase wavefront distortions and intensity scintillation that evolve into signal fading.

Adaptative Optics (AO) techniques can be used to improve the performance of laser communication links.¹² Its main task involves sensing the phase wavefront of the received beam and controlling the shape of a deformable mirror (DM), where the incoming beam is reflected, in order to compensate and minimize the phase distortions. This allows the focusing of the beam energy at the fiber core position. Adaptative Optics AO compensation of atmospheric turbulence has been identified as a key strategy in Free Space Optical Communications (FSOC).

To design the TOGS solution we considered three scenarios of transmission or reception QKD communications: a) Intercity, urban or interisland link, named as “Horizontal” links. b) LEO-to-Ground links, named as “Vertical” links c) Ground to sea or ground to aircraft We didn’t consider our TOGS design to transmit via GEO satellites, because for these links a telescope with a larger collecting area is needed. We have quoted the scenarios as “horizontal” and “vertical” indicating their approximated characteristics in relation to atmospheric turbulence because they will never be really horizontal or vertical.

3. TOGS SUBSYSTEMS FOR QKD BB84

We studied previous designs for optical communications ground station. Several iterations have been done before getting the final design suited to do QKD with transportability capability.

The implementation of the BB84 protocol¹⁰ has been done by using pulses with four polarizations equally distributed in a great circle of the poincare sphere. Four lasers are used in the transmitter to encode the bit value and measurement basis to obtain the states H,V,+45, and -45. The beams are combined in a non-polarizing beam splitter and dimmed in a variable optical attenuator. This quantum signal is combined with a beacon signal and sent to the telescope, which collimates the beam over free space towards Bob.

The receiver has a random beam splitter, which sets the measurement basis and polarizing beam splitters measure the value of the bit. A click on one of the photon-counting detectors set the bit value and base angle of measurement.

4. ATMOSPHERIC TURBULENCE AND ADAPTIVE OPTICS

One of the major weaknesses of the optical communications is that atmospheric turbulence introduces aberrations as phase changes to the transmitted beam due to local perturbations of the index of refraction of the air.¹³ If for a classical free-space optical communication the atmospheric turbulence is a problem, for quantum communications, that need to deal with very weak signals (single photon regime) is a real challenge. The diverging beam carrying the information after travelling for several kilometers from the emitter to the receiver, needs to be focused into a spot size equivalent to the size of the fiber core, that for a typical 1550nm SMF is of the order of 9μm. In

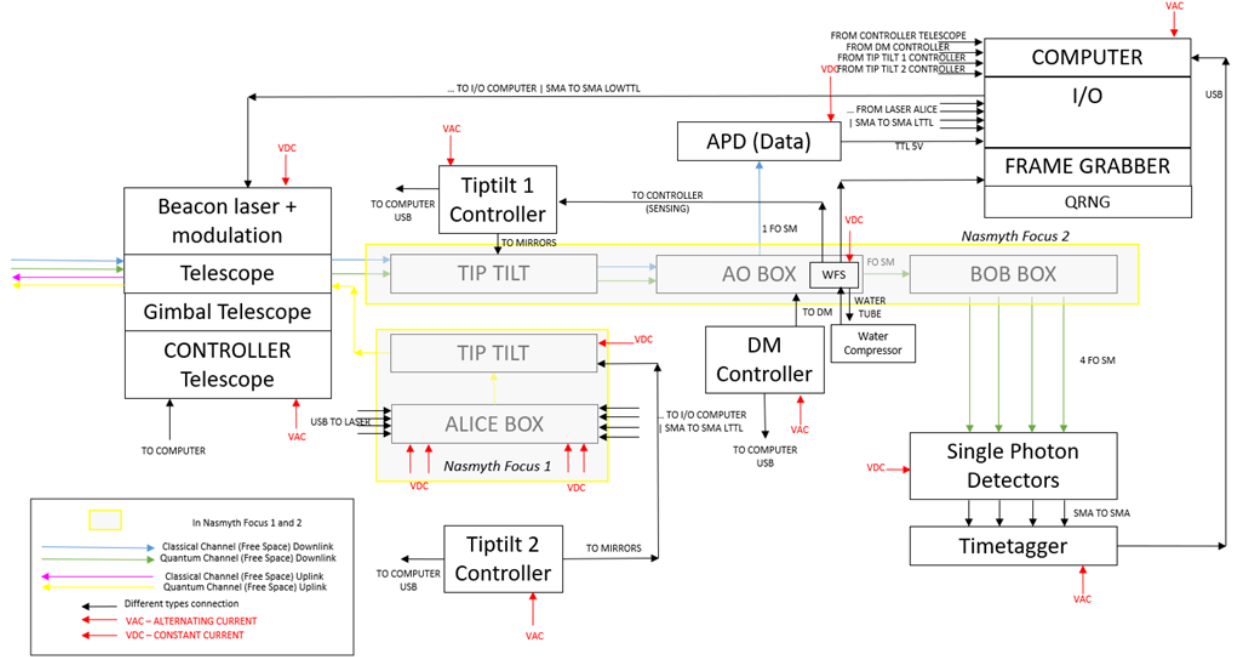


Figure 1: TOGS Subsystems

addition, a communication link as part of a permanent infrastructure has strong requirements concerning up-time operation and availability. It needs to operate during night and day-time in a 24/7 basis. Being day-time the most demanding scenarios, as the solar radiation introduces high noise to the communication. One of the possible solutions is given by adaptive optics. Unlike the adaptive optics systems used in large telescopes of the astronomical observatories, an adaptive optics system designed for optical communications is not an imaging system. The source (transmitting beam) is maintained on-axis thanks to a fine point and tracking system (PAT). A very useful parameter to characterize the strength of the atmospheric turbulence is the Fried parameter, given in equation 1:

$$r_0 = \left[0.423k^2 \int C_n^2(h) dh \right]^{-3/5}, \quad (1)$$

where $k = \frac{2\pi}{\lambda}$ is the wavenumber, and the C_n is the atmospheric turbulence strength profile. Typical values of the fried parameter for the scenarios considered are $r_0 = 3cm$ for a horizontal interurban link of a few kilometers and $r_0 = 5cm$ and $r_0 = 10cm$ or greater for a nocturnal LEO link with the receiver ground station located on Teide's observatory. If the atmosphere is modelled with a single layer of turbulent air with a velocity v , a characteristic frequency value corresponding to the atmosphere is given by the greenwood frequency (equation 2). As will be seen in section 5.3, this frequency determines the bandwidth of the system correction.

$$f_G = 0.427 \frac{v}{r_0} \quad (2)$$

5. ADAPTIVE OPTICS WITH PLENOPTIC WAVEFRONTSSENSOR

Superconducting nanowire detectors fed by single mode fibres are essential to minimize dark counts in a quantum communication receiver.¹⁴ Efficient coupling of the received light to the single mode fibre is fundamental for the system performance, but it gets deeply affected by the atmospheric turbulence.

Adaptive Optics measure and correct for the atmosphere effect on the light optimising the fibre coupling. All the parts of the AO system are fitted inside a box, except the controllers for the electronic devices. The box is limited in size and weight and will be closed and isolated to protect the optical elements inside. The main

elements of the system are a Fast steering mirror (FSM) to correct the Tip/tilt, a deformable mirror (DM) to correct higher order aberrations installed at the telescope exit pupil, a coupling relay to couple the light to a SMF fiber, a magnification relay for feeding signal to the wavefront sensor, and the plenoptic camera, consisting of an array of microlens mounted at the back focal length of an objective lens.

5.1 Plenoptic wavefront sensor

The plenoptic camera is based on a microlens array (similar to a Shack-Hartmann wavefront sensor (SH WFS)), but such an array is placed in the focus plane of the telescope and not in a pupil plane as demanded by a SH, resulting in a more simplified design, excluding the need of extra lenses to collimate the beam. The basic working principle is shown schematically in figure 8. This configuration generates at the camera sensor a collection of pupil images from as many viewpoints as microlenses are in the array. The pixels behind each microlens can be re-arranged to generate the aperture images. This is illustrated in figure 3. Finally, the wavefront slopes are extracted computing the relative displacement between the images obtained. In order that the subaperture images fill as much of the pupil as possible, but without interfering with each other, the microlens f-number should match exactly the f-number of the focusing system in front of it (see section 5.2). Hence another advantage of a plenoptic WFS over a SH configuration comes from the flexibility given by the possibility to change the sampling of the pupil, thanks to the pixel recombination. With a SH sensor, one should need to change the lenslet array if such a flexibility is wanted. Commented previously, an improvement in the coupling efficiency is expected to be obtained using a plenoptic WFS when compared to a SH, specially for strong turbulence.

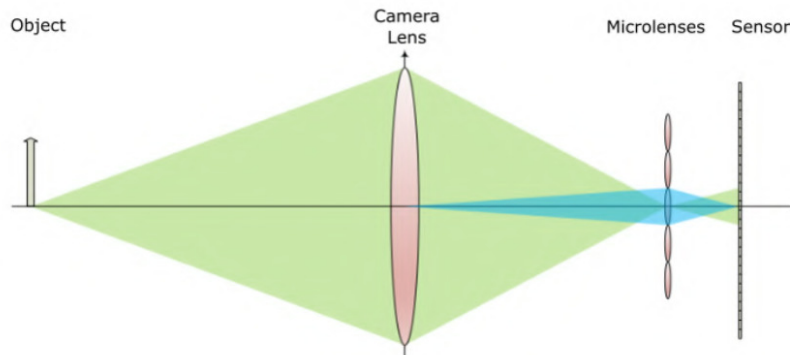


Figure 2: Illustration of the working principle of the plenoptic camera. The array of microlens is placed in the focus of the imaging lens. In green, the object image and in blue, is shown the aperture reimagination of the aperture by the central microlens

5.2 Design of the AO Subsystem

The design of the AO subsystem has the purpose to offer an active optics correction to the coupling into an SMF fiber for the QKD 1550nm quantum channel, while the correction, beacon and classical channel will be at 850nm. Figure 4 shows schematically the layout of the system.

The subsystem delivers an optical output through the coupling into an SMF. This fiber can be plugged easily to any kind of further instrumentation for use of the optical signal. To obtain a good performance and be able to work at diffraction limit, the diameter of the beam has been selected to be about 20mm, forcing the use of optics with an aperture twice the size of the beam. The compensation is done with two correcting elements: the tip/tilt platform mirror (TT) and the deformable mirror (DM). In the design is considered the DM97-25 from *Alpao*, that has 11 actuators across the aperture diagonal. The choice of the DM size and actuators has a consequence on the number of sub-apertures and the turbulence to compensate. With appropriate binning, the sensor of the camera will have 11 x 11 groups of pixels behind each microlens of the array. The system will incorporate a calibration source with an electrically controlled flipping mirror intercepting the beam path. Such a calibration source can be introduced and removed from the path at will. A beacon laser will be launched with

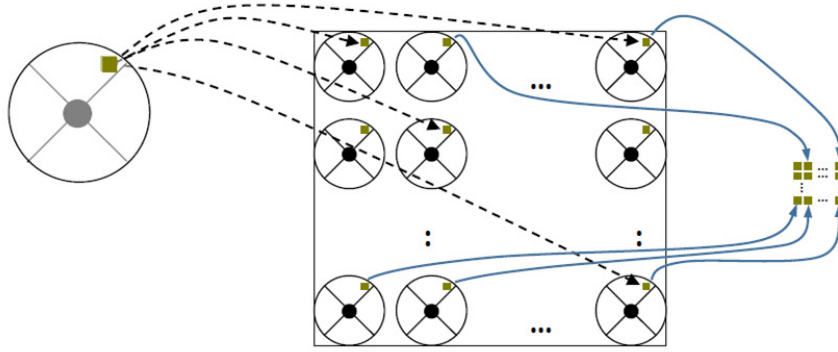


Figure 3: Illustration that shows how the process of a subaperture image is reconstructed. A viewpoint is indicated with the small green square. On the left is the position in the telescope pupil, in the middle is shown its position on every subaperture behind each microlens, and on the right the reconstructed position.

the system and is planned to be in the correction path, passing through the DM and TT before being launched with the telescope itself.

Because the Fried parameter in equation 1 has a dependency on the wavelength with $\lambda^{6/5}$, the correction is done using the shorter wavelength, specifically the beacon wavelength, that happens to be the same as the classical channel wavelength.

5.3 AO Subsystem performance

The AO subsystem has a narrow field of view of 60 arcsec. There is no need to form image, the subsystem will work on-axis. Active elements that will correct for the turbulence are a tip/tilt mirror (TT) and a deformable mirror (DM). Such elements rely on the ability of a WFS to detect the irregular and unpredictable phase changes of the beam introduced by the turbulence.

The two main contributors of phase error considered in the design are:

- a) The wavefront fitting error (given in equation 3), or the ability of the DM to provide necessary correction¹⁵

$$\sigma_F^2 = a_F \left(\frac{d}{r_0} \right)^{5/3}, \quad (3)$$

where $a_F = 0.287$

- b) The delay error given in equation 4, or the ability of the system to compensate in real time the rapid change on the turbulence.

$$\sigma_{TD} = \left(\frac{\tau_s}{\tau_0} \right)^{5/3}, \quad (4)$$

with τ_0 being related to the greenwood frequency (eq. 2) by $\tau_0 = 0.134/f_G$.

This two contributors mentioned give the maximum phase error of the wavefront that the system should have in order to work as expected. For this design the overall system performance should not be worse than $\lambda/6$ for $\lambda = 850nm$. Once this figure has been obtained for the system performance, following the same criteria, a tolerance analysis has also being performed. The system has been modelled and simulated in *OpticStudio*[®] substituting the DM with a flat mirror.

One of the design criteria for the system has been to use off-the-shelf lenses and optomechanical components in some cases to try to keep the overall cost of the system for a low budget without compromising the required

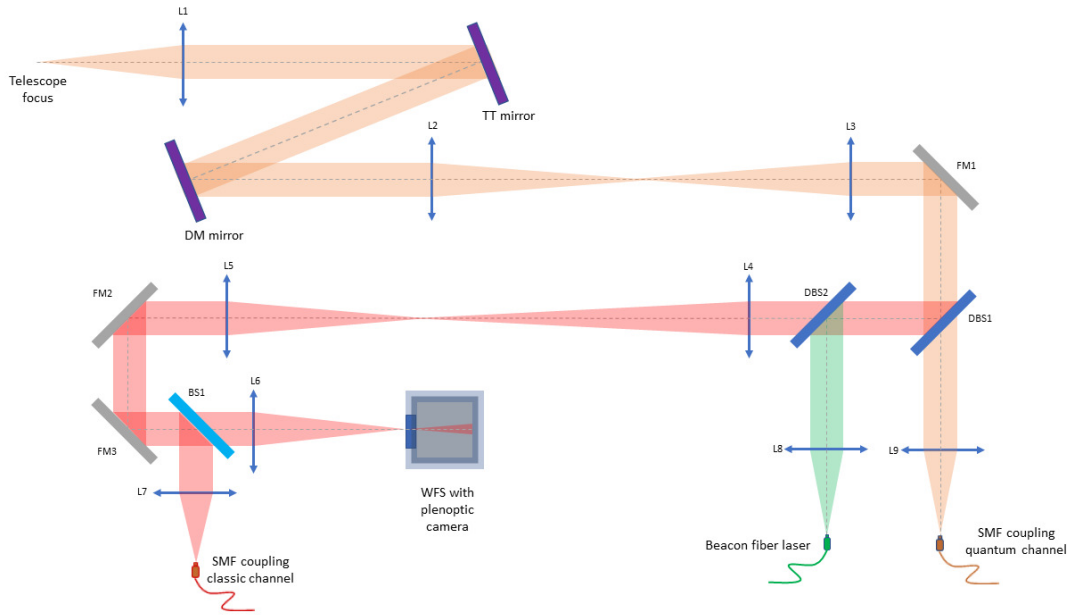


Figure 4: Schematic AO system layout

optical performance. The system has to be easy to align optically, inside the tight dimensions of the box, but should provide permanent and durable alignment.

It will be a transportable system that should be mounted on the telescope and set-up with certain agility to be operative within few hours. The overall dimensions are expected to fit inside a rectangular $900\text{mm} \times 600\text{mm}$ breadboard. Figure 5 gives an overview of the compacted appearance of the system inside a box. The box to be installed at the Nasmyth focus of the receiving/emitting telescope. The entry point of the beam from the telescope will be done through a hole on the breadboard.

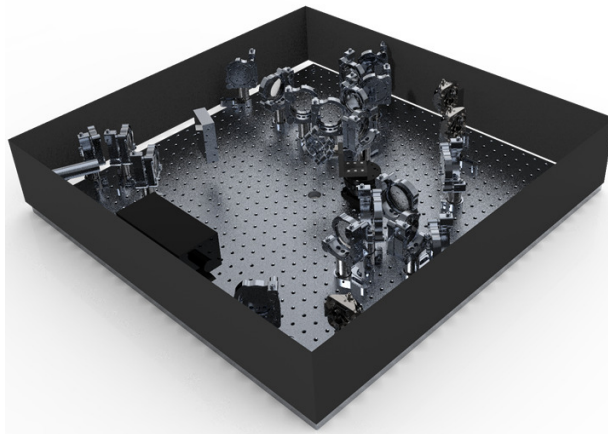


Figure 5: Render of the system showing the position and distribution of the elements inside a box. That box will be attached to the Nasmyth focus of the telescope. Note the central hole on the breadboard to allow the passing beam from Nasmyth focus.

The performance of the nominal system simulated in *OpticStudio*[®] is shown in figure 7, while the performance

stays within the desired bounds considering the worst tolerances.

5.4 Parameters

The table 2 gathers the main parameters of the system.

Table 2: Main parameters describing the optical system.

Microlens array	25x25 pitch $400\mu\text{m}$
DM	11 actuators in the diagonal
Field of view	60 arcsec (2.5 arcsec per microlens)
Receiver telescope	70cm aperture $f/12$ Ritchey-Chrétien 30% central obstruction
Camera sensor pixel	$9\mu\text{m}$ pixel pitch

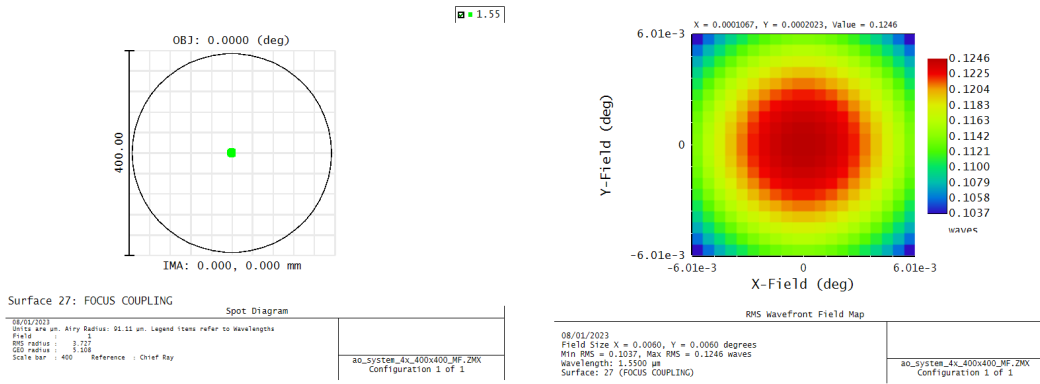


Figure 6: System performance: left - spot size at the coupling with SMF for 1550nm ; right - phase map at the plenoptic focus for 1550nm

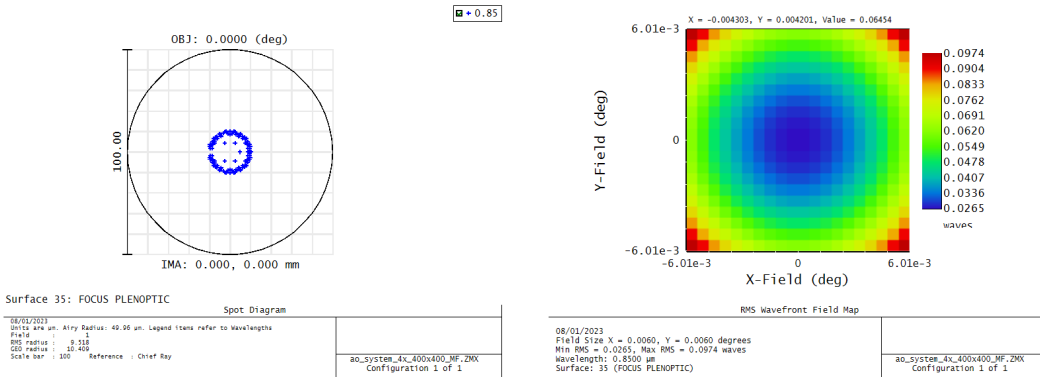


Figure 7: System performance: left - spot size at the coupling with SMF for 850nm ; right - phase map at the plenoptic focus for 850nm

6. SIMULATION FRAMEWORK

To analyze the performance of the plenoptic wavefront sensor over the Shack-Hartmann wavefront sensor, we use the Object-Oriented Matlab Adaptive Optics (OOMAO) Toolbox, to simulate the laser beam propagation

through the atmospheric turbulence and the effect of the adaptive optics compensation.¹⁶ In particular, the parameter used to evaluate the performance is the root mean square of the difference between the real and the measured wavefront phase. Our atmospheric turbulence has been defined in the Teide Observatory, with the refraction index structure constant Cn_2 and wind profiles measured on site, using scintillometers (SCIDAR at night and SHABAR during day time).¹⁷

We consider two scenarios in order to get the simulation of efficiency coupling light into a SMF:

- Scenario 1. The downlink from a GEO satellite to the transportable optical ground station (TOGS)
- Scenario 2. A ground-to-ground horizontal link along a 2 km path

It can be seen that in all the cases the plenoptic wavefront sensor measures the atmospheric turbulence with lower errors than the Shack-Hartmann sensor; although the difference in performance is not so big for the corresponding night operation regime. On the other hand, in strong daytime turbulence conditions, the plenoptic camera stands out as a much better performer, thus being a better candidate for wavefront sensing in a potential 24/7 adaptive optics system for optical communications.

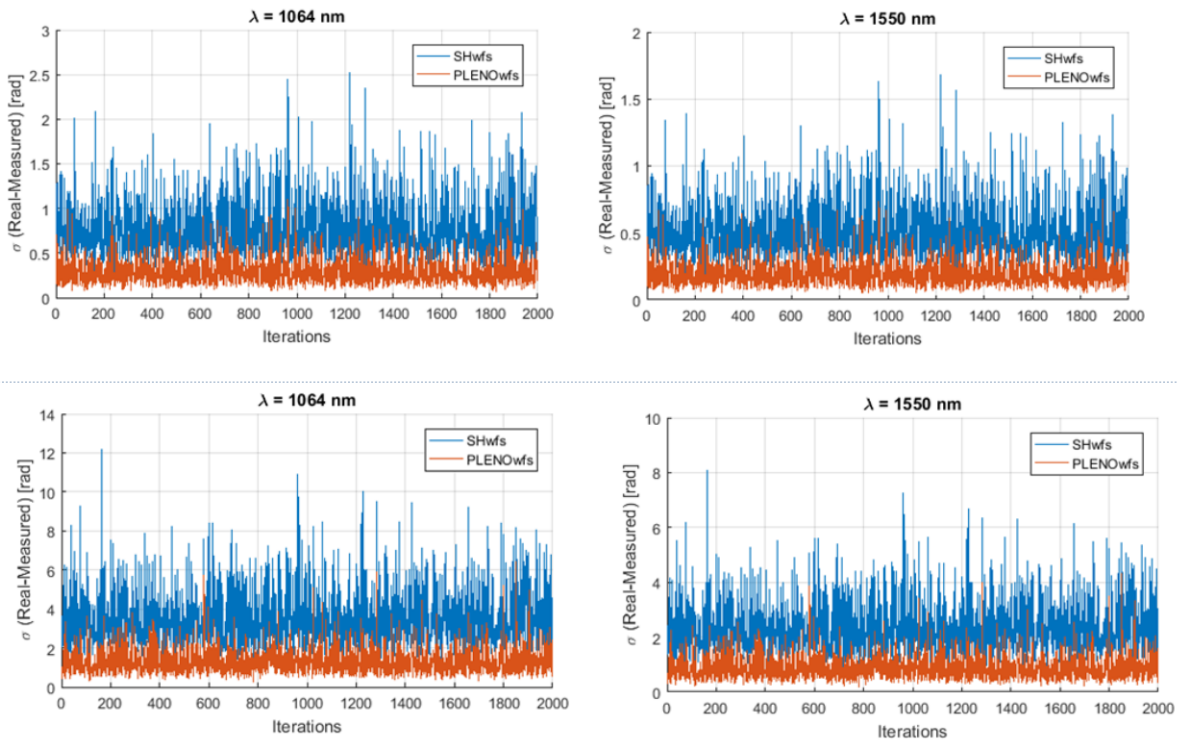


Figure 8: Performance comparison of the plenoptic wavefront sensor and the Shack-Hartmann wavefront sensor corresponding to the Night profile (top) and Day profile (bottom) using OGS as the receiver

7. CONCLUSIONS AND NEXT STEPS

In our design, we use Adaptive Optics in the receptor (Bob) to compensate the atmospheric turbulence and to get an efficient fiber coupling. Also we use a plenoptic wavefront sensor in order to improve wavefront correction with high atmospheric turbulence and to use the system in a 24/7 optical communications link. During 2023 and after the acquisition of several components, is expected to build a prototype at the optical bench in the facilities of IACTEC (technology transfer division of the IAC). In parallel to optical set-up, the control system will be developed within this period.

ACKNOWLEDGMENTS

The research and development described in this paper was carried out at the Instituto de Astrofísica de Canarias thanks to a financing of the refund and recovery funds of the European Union. The authors would like to acknowledge the contribution by Cabildo de Tenerife, for help in the "Capacitación tecnológica project".

REFERENCES

- [1] Rivest, R. L., Shamir, A., and Adleman, L., "A method for obtaining digital signatures and public-key cryptosystems," *Commun. ACM* **21**, 120–126 (feb 1978).
- [2] Kumar, A. and Garhwal, S., "State-of-the-Art Survey of Quantum Cryptography," *Archives of Computational Methods in Engineering* **28**(5), 3831–3868 (2021).
- [3] Trizna, A., O. A., "An overview of quantum key distribution protocols.," **21**(1) (2018).
- [4] Li, Y. M., Wang, X. Y., Bai, Z. L., Liu, W. Y., Yang, S. S., and Peng, K. C., "Continuous variable quantum key distribution," *Chinese Physics B* **26**(4), 1–7 (2017).
- [5] Schmitt-Manderbach, T., Weier, H., Fürst, M., Ursin, R., Tiefenbacher, F., Scheidl, T., Perdigues, J., Sodnik, Z., Kurtsiefer, C., Rarity, J. G., Zeilinger, A., and Weinfurter, H., *Experimental demonstration of free-space decoy-state quantum key distribution over 144 km*, PhD thesis (2007).
- [6] Trichili, A., Cox, M. A., Ooi, B. S., and Alouini, M.-S., "Roadmap to free space optics," *Journal of the Optical Society of America B* **37**(11), A184 (2020).
- [7] Chen, M., Liu, C., and Xian, H., "Experimental demonstration of single-mode fiber coupling over relatively strong turbulence with adaptive optics," *Applied Optics* **54**(29), 8722 (2015).
- [8] Fischer, E., Kudielka, K., Brady, A., Kamm, A., Berkefeld, T., and Ursin, R., "Modular adaptive optics solution for a QKD receiver on a fork mount telescope system," in [*International Conference on Space Optics — ICSO 2020*], Cugny, B., Sodnik, Z., and Karafolas, N., eds., **11852**, 118520X, International Society for Optics and Photonics, SPIE (2021).
- [9] Martinez, N., Ramos, L. F. R., Alonso, A., Montilla, I., and Torras, J., "Plenoptic wavefront sensor for free-space optical communications," in [*Free-Space Laser Communications XXXIV*], Hemmati, H. and Robinson, B. S., eds., **11993**, 119930T, International Society for Optics and Photonics, SPIE (2022).
- [10] Bennett, C. H., Brassard, G., and Mermin, N. D., "Quantum cryptography without bell's theorem," **68** (1992).
- [11] Shaik, K., "Atmospheric propagation effects relevant to optical communications," *The Telecommunications and Data Acquisition Report* (June 1988), 180–188 (1988).
- [12] Moll, F., "Conception and development of an adaptive optics testbed for free-space optical communication," **98** (2009).
- [13] Schwartz, N., Michau, M. V., Amra, M. C., Barthelemy, M. A., Vorontsov, M. M., Chazallet, M. F., and Velluet, M. M.-t., "Precompensation of turbulence effects by adaptive optics : application to free-space optics Publically Presented on the 17th of December 2009 before the jury composed of :," (2009).
- [14] You, L., "Superconducting nanowire single-photon detectors for quantum information," *Nanophotonics* **9**(9), 2673–2692 (2020).
- [15] Hardy, J. W., [*Adaptive Optics for Astronomical Telescopes*], Oxford University Press, New York, NY (1998).
- [16] Conan, R. and Correia, C., "Object-oriented Matlab adaptive optics toolbox," *Adaptive Optics Systems IV* **9148**(August 2014), 91486C (2014).
- [17] Montoya, L., De La Rosa, J. M., Castro-Almazán, J., Montilla, I., and Collados, M., "Modeling day time turbulence profiles: Application to teide observatory," *Adaptive Optics for Extremely Large Telescopes, 2017 AO4ELT5 2017-June* (2017).